

This is an Open Access document downloaded from ORCA, Cardiff University's institutional repository: <https://orca.cardiff.ac.uk/id/eprint/97716/>

This is the author's version of a work that was submitted to / accepted for publication.

Citation for final published version:

Harris, Kenneth David Maclean 2017. Explorations in the dynamics of crystalline solids and the evolution of crystal formation processes. *Israel Journal of Chemistry* 57 , pp. 154-170. 10.1002/ijch.201600088

Publishers page: <http://dx.doi.org/10.1002/ijch.201600088>

Please note:

Changes made as a result of publishing processes such as copy-editing, formatting and page numbers may not be reflected in this version. For the definitive version of this publication, please refer to the published source. You are advised to consult the publisher's version if you wish to cite this paper.

This version is being made available in accordance with publisher policies. See <http://orca.cf.ac.uk/policies.html> for usage policies. Copyright and moral rights for publications made available in ORCA are retained by the copyright holders.



Explorations in the Dynamics of Crystalline Solids and the Evolution of Crystal Formation Processes

Kenneth D. M. Harris*[a]

In honour of Professor Jack D. Dunitz FRS, on the 60th anniversary of establishing his research group at ETH, Zürich

Abstract: This article describes a few selected areas of (ammonium cyanate) that is not amenable to structural research within the field of structural chemistry, with characterization by single-crystal X-ray diffraction is also emphasis on aspects that have been influenced and inspired presented. On the theme of exploring the time evolution of by the seminal work of Jack Dunitz. The topics covered crystallization pathways, the recent development and application of in situ solid-state NMR techniques for mapping time-dependent changes that occur in the solid phase during include the study of dynamic properties of crystalline materials, focusing on the use of solid-state ^2H NMR spectroscopy to unravel details of dynamic hydrogen-bonding arrangements in crystalline alcohols and amino acids, as well as the use of in situ Raman microspectrometry to explore molecular transport processes through porous crystals. A case study involving the determination of both structural properties and dynamic properties of a material crystallization processes are discussed. Finally, the article contemplates the prospects for deriving a fundamental physicochemical understanding of crystal nucleation processes, which is identified as perhaps the most significant challenge in structural chemistry in the next few decades.

Keywords: crystal growth · Jack Dunitz · structural chemistry · dynamics of solids

1. Introduction

Although I had listened to many inspiring lectures by Jack Dunitz at conferences and had read several of his seminal publications, my first meeting with this great scientist was actually at an interview. In 1995, I had been encouraged to apply for the Chair of Structural Chemistry at the University of Birmingham, and one of the two external assessors for the appointment was Jack Dunitz. The interview process spanned two days. Jack was present on both days, so there was plenty of opportunity to enjoy talking about science with him, as well as facing his questions at the interview!

After moving to Birmingham, the next time I met Jack was at the ICCOSS meeting at Stony Brook, USA in 1997. While chatting to him after the conference dinner, he suggested that we should collaborate to determine the crystal structure of ammonium cyanate. Amazingly, in spite of the historical significance of this material, the crystal structure had never been previously reported. The problem was that single crystals of ammonium cyanate are impossible to prepare, so the only opportunity to determine the crystal structure would be to use powder diffraction data. Fortunately, my group was developing new techniques to determine the structures of organic materials from powder diffraction data (the subject of my lecture at Stony Brook), and Jack had clearly identified the opportunity to utilize our powder diffraction techniques to solve this long-standing, unresolved problem in structural chemistry. As an aside, one of Jack's remarkable characteristics, which I have come to realize over the years, is his

colossal knowledge of the literature, and his ability to make direct and meaningful connections between topical issues of the present day and work published in the long and distant past.

Although our first meeting took place as described above, my first "interaction" with the science of Jack Dunitz occurred much earlier. During my Ph.D. research in organic solid-state chemistry at the University of Cambridge, my supervisor (Sir John Meurig Thomas FRS) encouraged me to read the literature widely, and in particular, he pointed my reading in the direction of the work of Jack Dunitz. In addition to his seminal book,^[1] *X-ray Analysis and the Structure of Organic Molecules*, which was probably the most influential book in my process of learning the foundations of X-ray diffraction, I became very interested in the papers that he was publishing around that time^[2-4] on the physical interpretation of atomic displacement parameters (as determined in structure refinement from single-crystal X-ray diffraction data), especially as he was exploiting this information in imaginative ways to deduce insights into the dynamics of crystals. His 1988 paper^[3]

[a] K. D. M. Harris
School of Chemistry
Cardiff University
Park Place
Cardiff CF10 3AT (Wales) E-mail:
HarrisKDM@cardiff.ac.uk

1 with Schomaker and Trueblood in the *Journal of Physical*
2 *Chemistry* particularly captivated my scientific imagination. It
3 begins with the following sentences:

4 “The idea that atoms and molecules move in crystals –
5 indeed move sometimes with large amplitude – would have
6 struck most chemists of earlier generations as outlandish.
7 Professor Leopold Ruzicka once opined (to one of us) that “a
8 crystal is a chemical cemetery”. We know what he meant:
9 long rows of molecules, interred in a rigid geometrical
10 arrangement, lifeless compared with the molecular mazurkas
11 that can be imagined to occur in solution. The view that
12 Ruzicka expressed ... is perhaps still widely shared among
13 chemists and even (we suspect) among some crystallogra-
14 phers. It should not be.”

15 These sentences seemed to convey so convincingly the
16 necessity of giving due consideration to dynamic aspects of
17 solids (and perhaps convey even more convincingly the folly
18 of not doing so!). As in many other areas of structural
19 chemistry, it was clear from this paper, and his other
20 publications on similar topics, that Jack was striving to achieve
21 a much deeper physical understanding of the values of atomic
22 displacement parameters, when it seemed that many other
23 crystallographers were content instead to regard atomic
24 displacement parameters simply as a convenient means of
25 absorbing multiple errors in their refinements. Indeed, as
26 illustrated by this example, Jack always seems to be thinking
27 more deeply than others across the field of structural
28 chemistry, especially as his thinking is very firmly rooted in a
29 profound understanding of thermodynamics and other aspects
30 of physical chemistry.

31 Clearly, diffraction techniques have provided so much
32 information that has enriched our understanding of structure
33 across the full range of chemical, physical, biological, geo-
34 logical and materials sciences, but yet diffraction provides just
35 the time-averaged picture of a crystal. To search beyond this
36 time-averaged picture, we need to encompass other exper-
37 imental and computational techniques which reveal the time
38 dependence of structural properties across a range of different
39 timescales. Motivated by this quest, my group has been
40 interested over many years in exploring dynamic properties of
41 solids, especially using solid-state NMR spectroscopy, but also

incoherent quasi-elastic neutron scattering (IQNS) and molec-
ular dynamics simulations. Although such techniques reach
beyond the time-averaged description provided by diffraction
techniques, it is critical to recall that results from diffraction
experiments provide an essential constraint in the interpreta-
tion of data from these techniques, as the time average of the
correct dynamic model must agree with the time-averaged
structural description obtained from diffraction data.

As an illustration of some of the dynamic processes that can
occur in organic solids, Section 2 describes a few examples of
dynamic hydrogen-bonding arrangements that we have
explored using solid-state NMR techniques, and studies of
molecular translation through porous crystals studied by in situ
confocal Raman microspectrometry.

In Section 3, I return to consider the ammonium cyanate
system, covering both the crystal structure of this material
(Figure 1) determined from powder X-ray and neutron
diffraction data, the focus of our collaboration with Jack
Dunitz, and a subsequent investigation of the dynamic proper-
ties of this material.

Another aspect of crystalline materials that is critically
important in both fundamental and applied contexts is to
understand the fundamental processes underlying the forma-
tion and growth of crystals. In my opinion, the most significant
challenge in structural chemistry in the next few decades will
be to derive a fundamental physicochemical understanding of
the process of crystal nucleation (see Section 5), and then to
devise strategies to exploit this understanding to enable
crystallization processes to be controlled such that they are
directed towards very specific desired outcomes.

On a related theme of exploring the evolution of
crystallization pathways, much of our recent research has been
focused on the development and application of in situ solid-
state NMR techniques for mapping the time-dependent changes
that occur in the solid phase during crystallization (for example,
to identify the polymorphic form^[5–7] of the solid phase present
as a function of time, and to monitor the structural evolution of
the solid phase), as well as to unravel the corresponding
changes that occur in the liquid phase. Although our
experimental strategy is only able to explore the



Kenneth D.M. Harris graduated with a BSc degree in Chemistry from the University of St. Andrews (Scotland) in 1985, and then received a stimulating education in Solid-State Chemistry by carrying out research for his PhD degree under the supervision of Professor Sir John Meurig Thomas FRS at the University of Cambridge and at the Royal Institution, London between 1985 and 1988. After completing the PhD degree, he held positions as Lecturer in Physical Chemistry at the University of St. Andrews and then at University College London. He was appointed as Professor of Structural Chemistry at the University of Birmingham in 1995, and took up his present appointment as Distinguished Research Professor at Cardiff University in 2003. He has been awarded the Meldola (1991), Marlow (1996), Corday-Morgan (1999), Structural Chemistry (2001) and Tilden (2007/8) Medals of the Royal Society of Chemistry, and has been elected as a Fellow of the Royal Society of Edinburgh (2008), Fellow of the Learned Society of Wales (2011) and Member of Academia Europaea (2013). His research in the Physical Chemistry of Solids is focused on understanding fundamental aspects of the structural and dynamic properties of solids, and the development of experimental techniques for investigating these properties (particularly with regard to powder X-ray diffraction, solid-state NMR spectroscopy, and the new technique of X-ray Birefringence Imaging). He has held several appointments as Visiting Professor in Japan, France, U.S.A., Spain and Taiwan.

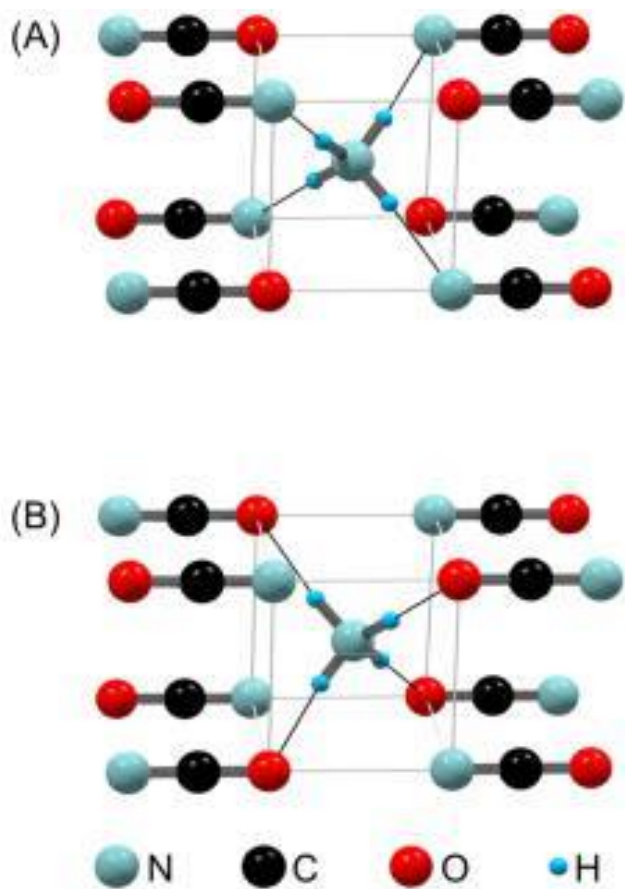


Figure 1. The crystal structure of ammonium cyanate. Two possible hydrogen-bonding arrangements are shown: (A) with the ammonium cation forming four N H...N hydrogen bonds; and (B) with the ammonium cation forming four N H...O hydrogen bonds. Powder neutron diffraction indicates that only hydrogen-bonding arrangement (A) exists in the crystal structure. Hydrogen bonds are shown as thin black lines.

crystallizing phase after the critical nucleation event has taken place, the technique can nevertheless yield significant insights into the sequence of events that occur at later stages along the crystallization pathway. Our recent work on the development and application of techniques in this field is summarized in Section 4.

Other aspects of the current research of my group, in particular our on-going development and application of techniques for structure determination of organic materials from powder X-ray diffraction data^[8] and our development of the new technique of X-ray birefringence imaging,^[9] are discussed in another article^[10] within this special issue.

2. Dynamic Properties of Crystalline Solids

2.1 Introduction

As conveyed so eloquently in the quotation of Jack Dunitz^[3] in Section 1, there is an unfortunate tendency (even among structural chemists) to regard crystalline solids as rigid assemblies of atoms or molecules, completely devoid of the interesting dynamic processes that occur for the same molecules and atoms when the solid is transformed into the molten or gaseous state, or when the crystalline solid is dissolved in solution. Conventional crystallographic models, so useful for displaying the fascinating arrangements of molecules and atoms in crystal structures, tend to convey the impression that the molecules and atoms are fixed rigidly in place, each constrained to reside motionlessly in its assigned position within the architecture of the crystal. But the molecules and atoms in a crystalline solid are certainly not motionless – they are dynamic entities, whether through small amplitude vibrational motions about their equilibrium positions or, in some cases, through large-scale reorientational motions, chemical exchange processes, or diffusion of molecules through crystals. Clearly, the occurrence of dynamic processes may have a significant influence on the physical properties of crystalline materials (including properties that may underpin materials applications, such as optical, electrical and magnetic properties). Thus, to derive a fundamental understanding of the properties of a material, it is essential not only to consider the time-averaged crystal structure, as revealed by diffraction-based techniques, but also to consider the time dependence of the crystal structure, as described by the variety of dynamic processes that can occur across a range of timescales.

Several experimental and computational techniques, including solid-state NMR spectroscopy, incoherent quasielastic neutron scattering, molecular dynamics simulation, Raman scattering, Brillouin scattering, and dielectric relaxation can probe the dynamic properties of solids, with each technique appropriate for studying dynamic processes occurring on a particular characteristic timescale. Among these techniques, solid-state NMR^[11, 12] is particularly powerful, since by judicious choice of the specific NMR-active nucleus and the specific NMR phenomenon to be investigated, detailed information on a wide range of different types of dynamic process, occurring over a wide range of timescales, can be established. These dynamic processes include intramolecular dynamics (such as interconversion of a molecule between different conformations, rotation about bonds, and dynamic tautomerism), as well as reorientational motions of the whole molecule (as observed for guest molecules in solid inclusion compounds and for molecules in other rotator phase solids). In many cases, more than one type of dynamic process may occur in the material, often at different rates, and each process may be studied selectively by appropriate choice of NMR techniques. This section gives a few illustrative examples of some types of dynamic process that can occur in crystalline organic solids,

2 highlighting the application of solid-state NMR techniques
3 (particularly broad-line ^2H NMR) to probe these processes.

4 **2.2 Dynamics of Hydrogen-Bonding Arrangements 5 Revealed by Solid-state ^2H NMR Spectroscopy**

6 **2.2.1 Brief Background to Solid-state ^2H NMR**

10 Solid-state ^2H NMR is a powerful technique for studying
11 reorientational motions of molecules in solids,^[12–17] and has
12 been used to characterize the dynamic properties of a wide
13 range of systems. Different aspects of solid-state ^2H NMR
14 yield different information on dynamic properties, and the two
15 most commonly used techniques are ^2H NMR line-shape
16 analysis and ^2H NMR spin-lattice relaxation time measure-
17 ments.

18 For ^2H nuclei in organic solids, the quadrupolar interaction
19 is normally so large that other nuclear spin interactions are
20 negligible in comparison. A polycrystalline powder sample
21 containing a random distribution of crystal orientations gives a
22 characteristic ^2H NMR “powder pattern” (several examples of
23 which are shown in figures below). Analysis of the ^2H NMR
24 powder pattern allows quantitative determination of the
25 quadrupole interaction parameters (the quadrupole coupling
26 constant c and the asymmetry parameter η) for the ^2H nucleus.

27 As the quadrupole interaction parameters are influenced
28 significantly when the ^2H nucleus undergoes motion on an
29 appropriate timescale (see below), the appearance of the
30 ^2H NMR powder pattern changes significantly, depending on
31 the rate and mechanism of the motion. When the ^2H nucleus is
32 static, or undergoes rates of motion lower than ca. 10^3 s^{-1} (the
33 static/slow motion regime), the ^2H NMR line shape has a

34 characteristic shape that is independent of the rate and
35 geometry of the motion. ^2H NMR line-shape analysis is
36 particularly informative when the rate of motion is in the range
37 10^3 s^{-1} to 10^8 s^{-1} (the intermediate motion regime), as analysis
38 of the ^2H NMR line shape in this regime provides detailed
39 information on the rate and mechanism of the dynamic
40 process. For rates of motion higher than ca. 10^8 s^{-1} (the rapid
41 motion regime), the actual rate of motion cannot be
42 established from ^2H NMR line-shape analysis, but information
43 on the geometry and mechanism of the motion can still be
44 obtained. ^2H NMR line-shape analysis is generally carried out
45 by calculating the line shapes for proposed dynamic models,
46 and finding the dynamic model for which the set of calculated
47 line shapes give rise to the best fit to the set of experimental
48 line shapes recorded as a function of temperature. When the
49 rate of motion is in the rapid regime with respect to ^2H NMR
50 line-shape analysis, detailed dynamic information may also be
51 obtained from measurement and analysis of the ^2H NMR spin-
52 lattice relaxation time (T_1), which is particularly sensitive for
53 studying dynamic processes with rates in the range 10^3 to
54 10^8 (where ω is the ^2H Larmor frequency).

Solid-state ^2H NMR has been used widely to study
molecular dynamics in materials, including dynamics of
rotator phase solids (plastic crystals), the dynamics of guest
molecules in crystalline inclusion environments, reorienta-
tional motions of individual functional groups, and the
motional properties of polymers and membranes.

7 **2.2.2 Hydrogen-Bond Dynamics in Crystalline Amino 8 Acids**

Crystalline forms of the proteinogenic amino acids have often
been used as model compounds for probing functional group
interactions in proteins. In the crystalline state, the amino acids
exist (in general) in the zwitterionic form $[\text{RR}'\text{C}(\text{NH}_3^+)(\text{CO}_2^-)]$, and the ammonium (NH_3^+) group is often engaged in three
intermolecular $\text{N}-\text{H}\cdots\text{O}$ hydrogen bonds. In such cases, the
crystal structures established from X-ray diffraction look
perfectly ordered in every aspect, and the possibility that the C
 NH_3^+ group may actually undergo a 3-site 120° jump motion
about the C-N bond is “hidden” from the diffraction data
because the local symmetry of the dynamic process matches the
local symmetry of the dynamic moiety (in this case, local 3-fold
symmetry). We note that a 3-site 120° jump motion implies
that the C- NH_3^+ group has a specific residence time (τ) in a
particular orientation, followed by an essentially instantaneous
jump (by 120° rotation about the C-N bond) to an identical
orientation, and so on. The time average over this jump motion
(for which the rotation frequency is $\nu = (3\tau)^{-1}$) is identical to the
static situation, and the crystal structure determined from
diffraction data reveals no evidence for the existence of any
disorder.

Similarly, the crystal structure of urea determined from
diffraction data^[18–20] looks completely ordered, and does not
reveal the fact that the urea molecule actually undergoes a 2-
site 180° jump motion about the C=O bond axis (with the 2-
fold symmetry of the jump process matching the 2-fold
symmetry of the urea molecule).^[21–24] Again, solid-state
 ^2H NMR was a powerful technique for establishing the
occurrence of the dynamic process in this case.

Focusing on crystalline amino acids, solid-state ^2H NMR
techniques have been applied^[25] to establish the dynamics of
ammonium group reorientation in samples of the α polymorph
and β polymorph of L-glutamic acid $[\text{HO}_2\text{CCH}_2\text{CH}_2\text{CH}(\text{NH}_3^+)(\text{CO}_2^-)]$ deuterated in the ammonium group (i. e., ND_3^+). The
fact that the solid-state ^2H NMR spectrum of each polymorph
changes significantly as a function of temperature (see Figure
2 and Figure 3) reveals clearly that the C- ND_3^+ groups are
dynamic. In the crystal structure of each polymorph,
determined from single-crystal neutron diffraction data,^[26, 27]
the C- ND_3^+ group forms three intermolecular $\text{N}-\text{D}\cdots\text{O}$
hydrogen bonds. The changes in the experimental ^2H NMR
spectra as a function of temperature are completely described
by the 3-site 120° jump model discussed above. From the best-
fit simulated ^2H NMR spectrum corresponding to each
experimental ^2H NMR spectrum, the rate (k) of the 3-

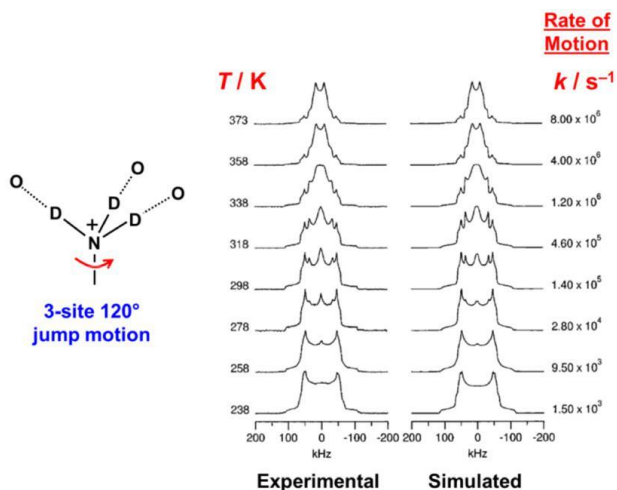


Figure 2. Experimental solid-state ^2H NMR spectra recorded as a function of temperature for a powder sample of the α polymorph of deuterated L-glutamic acid, and the best-fit simulated solid-state ^2H NMR spectrum at each temperature, calculated for the dynamic model (3-site 120 $^\circ$ jump motion of the ND_3^+ group). A schematic of the dynamic model is shown at the left.

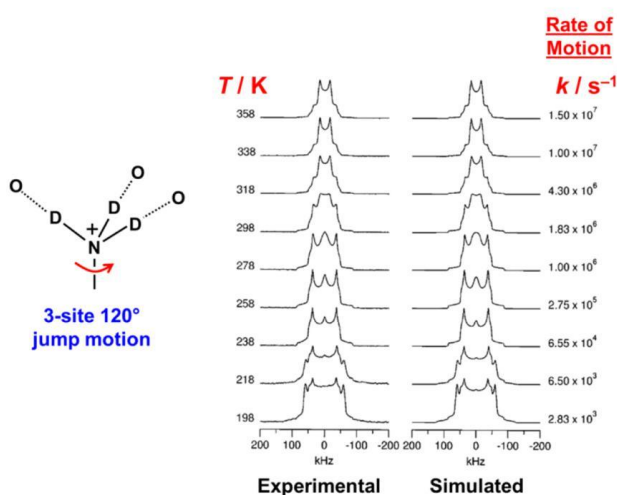


Figure 3. Experimental solid-state ^2H NMR spectra recorded as a function of temperature for a powder sample of the β polymorph of deuterated L-glutamic acid, and the best-fit simulated solid-state ^2H NMR spectrum at each temperature, calculated for the dynamic model (3-site 120 $^\circ$ jump motion of the ND_3^+ group). A schematic of the dynamic model is shown at the left.

site 120 $^\circ$ jump motion is established at each temperature studied (see Figures 2 and 3).

From Figures 2 and 3, it is clear that there are significant differences in the rate of the ND_3^+ group reorientation (at a given temperature) in the two polymorphs. On the assumption of Arrhenius behaviour for the temperature dependence of the rate of reorientation of the ND_3^+ group (Figure 4), the activation energy for this motion was determined to be (47

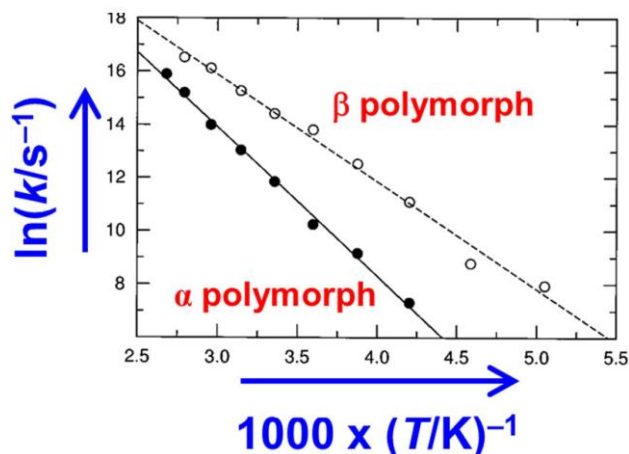


Figure 4. Arrhenius plots for the 3-site 120 $^\circ$ jump motion of the ND_3^+ group in the α polymorph (filled circles) and β polymorph (open circles) of deuterated L-glutamic acid, determined from best-fit simulations of the ^2H NMR line shapes shown in Figures 2 and 3. The straight lines are linear least-squares fits.

2) kJ mol^{-1} for the α polymorph and (34 \pm 3) kJ mol^{-1} for the β polymorph, in good agreement with results from ^1H NMR spin-lattice relaxation time data, from which the activation energy was established to be (48 \pm 1) kJ mol^{-1} for the α polymorph and (39 \pm 2) kJ mol^{-1} for the β polymorph. In the crystal structures of the α and β polymorphs,^[26, 27] there are only small differences in the distances and angles that define the hydrogen-bond geometries in the two polymorphs. However, these small differences in hydrogen-bonding geometries involving the ND_3^+ group suggest that the hydrogen bonding is stronger in the α polymorph, consistent with the observation from our ^2H NMR study that the activation energy for the ammonium group reorientation is higher for the α polymorph.

Another interesting issue for proteinogenic amino acids is to compare the properties of racemic and enantiomerically pure crystalline forms.^[28] With regard to dynamic properties, solid-state ^2H NMR studies have been carried out^[29] on the racemic and enantiomerically pure crystalline forms of serine [$\text{HOCH}_2\text{CH}(\text{NH}_3^+)(\text{CO}_2^-)$], for samples of DL-serine and L-serine deuterated in the ammonium group. For both L-serine and DL-serine, ^2H NMR line-shape analysis indicates that the ND_3^+ group undergoes a 3-site 120 $^\circ$ jump motion. At a given temperature, the jump frequency (k) is substantially higher for L-serine (for example, at 233 K, $k = 5.0 \pm 10^6 \text{ s}^{-1}$ for L-serine and $k = 6.0 \pm 10^4 \text{ s}^{-1}$ for DL-serine). The results from both ^2H NMR line-shape analysis (LA) and ^2H NMR spin-lattice relaxation time measurements (SLR) indicate that the

activation energy for the 3-site 120 $^\circ$ jump motion of the ND_3^+ group is significantly higher for DL-serine (38.0 kJ mol^{-1} (LA); 39.7 \pm 0.81 kJ mol^{-1} (SLR)) than for L-serine (23.4 \pm 0.8 kJ mol^{-1} (LA); 23.8 \pm 0.3 kJ mol^{-1} (SLR)), suggesting that the hydrogen bonding involving the ND_3^+ group may be significantly stronger in the case of the racemic material.

1 The effects of hydrogen bonding on ammonium group
2 dynamics have also been studied in several other crystalline
3 amino acids.^[30–32]

4 It is relevant to ponder the extent to which these significant
5 differences in rotational frequencies of functional groups may
6 contribute to differences in the entropies of the different
7 crystal forms under comparison, and hence may contribute to
8 differences in their Gibbs energies. Given the considerable
9 current interest (see Section 5) in computational studies to
10 assess the relative energies of different solid forms of
11 materials (e. g., different polymorphs, or racemic versus
12 enantiomerically pure forms), it is important to consider
13 whether differences in rotational dynamics of functional
14 groups may influence the ranking of structures based on Gibbs
15 energies. Given that the existence of certain motions (such as
16 the 3-site 1208 jump motion of ammonium groups in amino
17 acids) is not even revealed by diffraction techniques, and to
18 establish the rates of such motions requires detailed spectro-

19 scopic studies (such as the ²H NMR studies described above),
20 it is clear that standard computational approaches to assess
21 energetic properties of crystalline solids based purely on
22 consideration of time-averaged crystal structures may be
23 missing certain factors that could have an important influence
24 on the relative energetic ordering of different crystalline
25 forms.

28 2.2.3 Hydrogen-Bond Switching in Crystalline 29 Alcohols

30 In the crystal structure of triphenylmethanol (Ph₃COH),^[33] the
31 molecules form hydrogen-bonded “tetramers”, with the oxy-
32 gen atoms positioned approximately at the corners of a
33 tetrahedron (Figure 5). The point symmetry of the tetramer is
34 C₃ (rather than T_d); thus, three Ph₃COH molecules (denoted
35 “basal”) are related to each other by a 3-fold rotation axis, and
36 the other molecule (denoted “apical”) lies on this axis. Thus,
37 the oxygen atoms from the four molecules in the tetramer
38 form a pyramidal arrangement with an equilateral triangular
39 base, and the O···O distances (ca. 2.9 Å) are consistent with
40 the tetramer being held together by O H···O hydrogen bonds.
41 As there are six O···O edges of the tetramer but only four
42 O H···O hydrogen bonds, there are several different permuta-
43 tions for arranging the O H···O hydrogen bonds, and disorder
44 of the hydrogen-bonding arrangement may be anticipated,
45 consistent with the fact that hydrogen-atom positions were not
46 reported for the hydroxyl groups in the crystal structure

47 determined from single-crystal X-ray diffraction data at
48 ambient temperature. To explore whether the disorder of the
49 hydrogen-bonding arrangement is dynamic, solid-state
50 ²H NMR studies were carried out^[34] on the selectively
51 deuterated material Ph₃COD.

52 The solid-state ²H NMR line shape for Ph₃COD varies
53 significantly as a function of temperature,^[34] indicating that
54 the hydrogen-bonding arrangement is dynamic. Several plau-
55 sible dynamic models were considered, and it was found that
56 only one model gives a good fit to the experimental solid-state

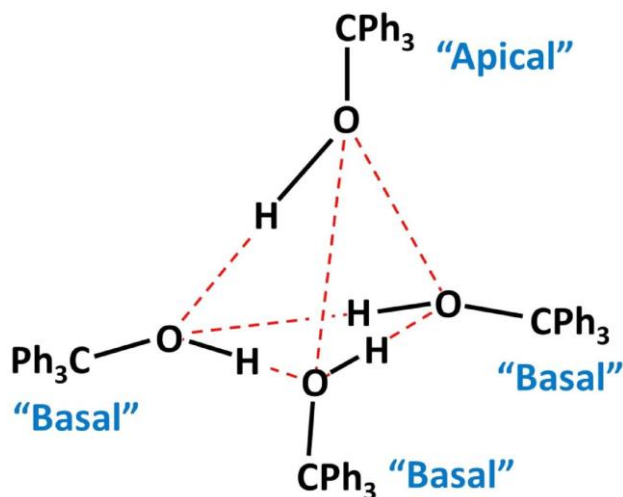


Figure 5. Schematic representation of the hydrogen-bonded “tetramer” in the crystal structure of triphenylmethanol. The hydrogen-bonding arrangement shown is only one of several possible hydrogen-bonding arrangements for the tetramer. The unique “apical” molecule and the three “basal” molecules are discussed in the text in the context of the dynamic model for hydrogen-bond switching.

²H NMR spectra across the full temperature range studied. In this model, the deuteron of the apical molecule undergoes a 3-site 1208 jump motion by rotation about the C O bond, with equal populations of the three sites, whereas the deuterons of the three basal molecules undergo 2-site 1208 jumps, by rotation about their C O bonds. In addition, each deuteron undergoes rapid libration about the relevant C O bond, with the libration amplitude increasing as a function of temperature. The behaviour of the basal molecules is interpreted in terms of the existence of two possible hydrogen-bonding arrangements (clockwise and anticlockwise) on the basal plane of the pyramid. The 2-site 1208 jump motion for the basal molecules “switches” between these two hydrogen-bonding arrangements, requiring correlated jumps of the hydroxyl groups of all three basal molecules. On the assumption of Arrhenius behaviour for the temperature dependence of the jump frequencies, the activation energies for the jump motions were determined to be 10 kJ mol⁻¹ for the apical deuteron and 21 kJ mol⁻¹ for the basal deuterons. This dynamic model is further supported by consideration of ²H NMR spin-lattice relaxation time data.

Subsequent studies included a detailed analysis of the disordered hydrogen-bonding arrangement in triphenylmethanol using single-crystal neutron diffraction^[35] and an investigation of the contrasting hydrogen-bond dynamics in the silicon analogue triphenylsilanol using solid-state ²H NMR.^[36] A theoretical study of the pathways for hydrogen-bond switching in a geometrically similar model system, comprising a tetrahedral hydrogen-bonded arrangement of methanol molecules, has also been reported.^[37]

Molecular Transport Through Porous Organic 2.3 Crystals

Many types of solid inclusion compound (for example, zeolites, aluminophosphates, and metal-organic frameworks) have important applications in molecular separation processes, based on the fact that selective incorporation and exchange of guest molecules of differing size and shape can occur, while

retaining the integrity of the host structure. Transport processes of molecules through the systems of interconnected tunnels and cages in such materials have been widely studied, and can be a critical factor in developing successful applications of these materials. For example, in applications of zeolites based on catalytic transformations or separation processes, the rate of diffusion of guest molecules within the zeolitic host structure^[38, 39] may have an important bearing on the overall rate of the process.

For solid organic inclusion compounds, on the other hand, there are relatively few examples in which the crystal integrity of the host structure is maintained when the guest molecules are lost from the inclusion compound, thus limiting the prospects for carrying out guest exchange processes that proceed via the “empty” host structure. Nevertheless, a process for achieving guest exchange in such cases, by a mechanism that does not proceed via the empty host tunnel structure, has been identified^[40] and has been demonstrated in the case of urea inclusion compounds.

Urea inclusion compounds are an extensively studied family of solid organic inclusion compounds,^[41–45] in which linear-chain guest molecules (based on a long n-alkane chain) are arranged along one-dimensional tunnels (diameter ca. 5.25 Å) that exist within the urea host structure, which is constructed from a helical hydrogen-bonded arrangement of urea molecules (Figure 6). The fact that the urea tunnel structure is stable only when it is filled with a dense packing of guest molecules imposes a limitation on the opportunity to

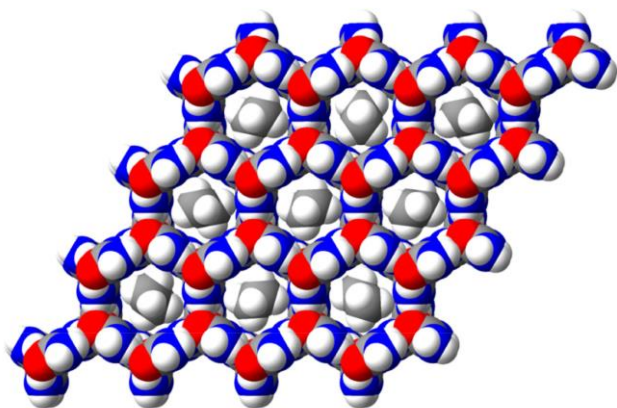


Figure 6. Crystal structure of the hexadecane/urea inclusion compound at ambient temperature, showing nine complete tunnels (with van der Waals radii) viewed along the tunnel axis. The hexadecane guest molecules have been inserted into the tunnels, illustrating orientational disorder.

develop potential applications based on molecular adsorption and/or molecular separation, analogous to the types of process that have been exploited for zeolitic host materials.

The proposed mechanism for guest exchange^[40] (see Figure 7) is based on the requirement that the host tunnels remain fully occupied by guest molecules throughout the exchange process, but with the identity of the guest molecules changing as a function of time. The idea is that net transport of guest molecules in one direction along the host tunnel can be achieved by inserting “new” (thermodynamically more favourable) guest molecules at one end of a crystal of the inclusion compound (e. g., by dipping the crystal into the liquid phase of the new guest), with the “original” guest molecules expelled from the other end of the crystal.

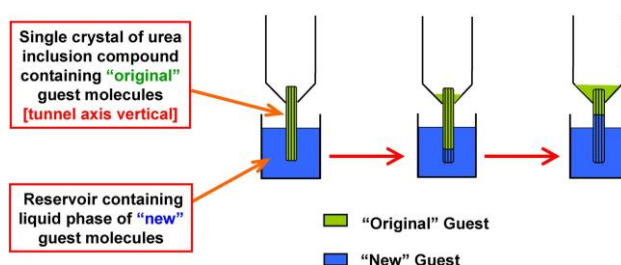


Figure 7. Mechanism for guest exchange in a single crystal of a urea inclusion compound. In the single crystal shown, the tunnels in the urea host structure are vertical.

The successful implementation of this guest exchange process has been demonstrated^[40] in the case of urea inclusion compounds. To gain deeper insights into this process, confocal Raman microspectrometry has been exploited^[46] as an in situ probe (Figure 8) to yield information on the spatial distribution of the original and new guest molecules within the crystal, and to establish how the spatial distribution of the original and new guest molecules changes as a function of time. The published work in this area has focused on using the 1,8-dibromooctane/urea inclusion compound as the “original”

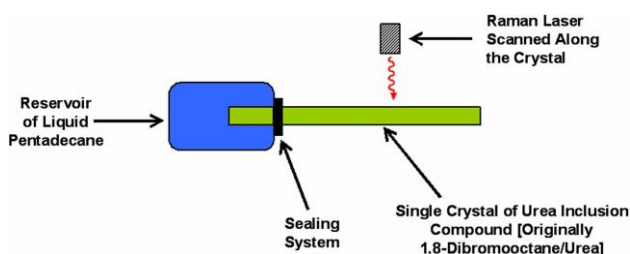
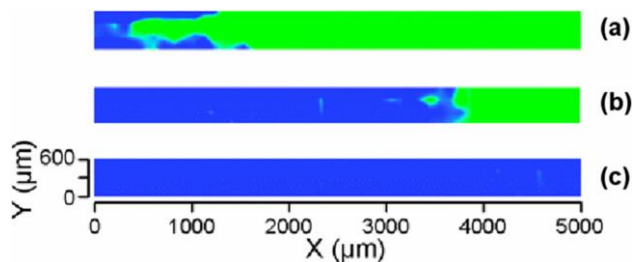


Figure 8. Schematic of the experimental assembly for in situ Raman microspectrometry studies of guest exchange in a urea inclusion compound, comprising the single crystal of the urea inclusion compound (green), initially containing 1,8-dibromooctane guest molecules, attached to a reservoir containing liquid pentadecane (blue).

1 crystal and pentadecane as the “new” type of guest molecule.
 2 For this system, analysis of the Raman microspectrometry
 3 data is based^[46] on studying the variation of the intensity of the
 4 C Br stretching band of the original 1,8-dibromooctane guest 5
 molecules (for the predominant trans end-group conformation) 6 as
 a function of position in the crystal and as a function of
 7 time (Figure 9). Such data provide quantitative information on
 8 kinetic and mechanistic aspects of the transport of guest
 9 molecules through the host tunnel structure during the guest
 10 exchange process,^[47] revealing inter alia that unidirectional
 11 transport of guest molecules in this system occurs at a constant
 12 rate of ca. $(70.3 \pm 2.2) \text{ nm s}^{-1}$ at ambient temperature. Fur-
 13 thermore, in situ studies using confocal Raman microspectrometry^[48]
 14 have revealed that the guest exchange process is
 15 associated with significant changes in the conformational
 16 properties of the original (1,8-dibromooctane) guest molecules
 17 within the “boundary region” between the original and new
 18 guests, corresponding to a significant increase in the propor-
 19 tion of 1,8-dibromooctane guest molecules with the gauche
 20 end-group conformation. In addition, bi-directional transport
 21 of guest molecules through the urea tunnel structure has been
 22 demonstrated, and mechanistic details of this process have
 23 been rationalized.^[49] At this stage, several fundamental aspects
 24 relating to such guest exchange processes remain to be
 25 understood; for example, studies to probe the temperature
 26 dependence of the rate of transport, and hence to establish
 27 activation parameters for the transport process, have not yet
 28 been reported. However, establishing an understanding of the
 29 fundamentals of guest exchange processes in such materials is
 30 a prerequisite for developing and optimizing a range of
 31 potential applications in molecular separation, based for
 32 example on discrimination of molecular size, shape, and
 33 chirality.



47 **Figure 9.** Results from time-resolved and spatially resolved
 monitoring of guest exchange in a single crystal of a urea
 inclusion compound using in situ Raman microspectrometry. The
 Raman micrographs were recorded during transport of
 pentadecane molecules into and along the tunnels, displacing
 the guest molecules (1,8-dibromooctane) originally present.
 The probed region shown represents only part of the crystal,
 and the transport of guest molecules occurs from left to right
 (the tunnels run horizontally in the micrographs shown).
 Regions coloured blue are rich in pentadecane and regions
 coloured green are rich in 1,8-dibromooctane. The time taken
 to record each micrograph was ca. 28 mins; the three micrographs
 shown were recorded: (a) 18 hrs; (b) 29 hrs; and (c) 40 hrs
 after commencing the guest exchange process.

3. Structure and Dynamics of Ammonium Cyanate: Collaboration with Jack Dunitz and Beyond

3.1 Introduction

In 1828, Friedrich Woehler^[50] observed, while attempting to
 prepare ammonium cyanate $[\text{NH}_4^+ \text{OCN}^-]$ by a number of
 different routes, that urea $[\text{O}=\text{C}(\text{NH}_2)_2]$ was formed instead.
 Subsequently, Woehler and Liebig^[51] were successful in
 preparing solid ammonium cyanate, and demonstrated that,
 under appropriate conditions, this material undergoes a solid-
 state reaction to produce urea. These discoveries played a
 seminal role in the history of chemistry, as the reaction from
 ammonium cyanate to urea represented the first direct evidence
 that it is possible for an inorganic material to be converted into
 an organic substance that was known to occur in living systems.
 Subsequently, this reaction has received much attention, both in
 aqueous solution and in the solid state,^[52] although most
 experimental studies have focused on the reaction in solution.

3.2 Structural Properties

In spite of the importance of understanding structural prop-
 erties of ammonium cyanate in the solid state, structure
 determination by single-crystal X-ray diffraction was pre-
 cluded by the fact that this material can be prepared only as a
 microcrystalline powder.

Structure determination was carried out initially from
 powder X-ray diffraction data,^[53] which established the
 positions of the non-hydrogen atoms, but could not reliably
 distinguish the orientation of the ammonium cation (as a
 consequence of the low X-ray scattering power of hydrogen).
 Subsequent powder neutron diffraction studies^[54] were neces-
 sary to establish details of the hydrogen-bonding arrangement,
 as discussed below. The structure is tetragonal with space group
 $P4/nmm$. The nitrogen atom of the ammonium cation is located
 at the centre of a nearly cubic local arrangement of oxygen and
 nitrogen atoms (from cyanate anions), which occupy alternate
 corners of the “cube”. Two plausible orientations of the
 ammonium cation may be proposed, in one case forming four
 $\text{N}^{\text{H}} \cdots \text{O}$ hydrogen bonds, and in the other case forming four
 $\text{N}^{\text{H}} \cdots \text{N}$ hydrogen bonds (Figure 1). Powder neutron diffraction
 studies^[54] on the deuterated material $\text{ND}_4^+ \text{OCN}^-$ (actually with
 a percentage deuteration of ca. 77–81 %) definitively support
 the structure with $\text{N}^{\text{D}} \cdots \text{N}$ hydrogen bonding, with no
 detectable extent of disorder between the $\text{N}^{\text{D}} \cdots \text{O}$ and
 $\text{N}^{\text{D}} \cdots \text{N}$ hydrogen-bonding arrangements. Thus, Rietveld
 refinement calculations for a structural model comprising both
 orientations of the ammonium cation with fractional occupancies
 x and $(1-x)$, respectively, converge towards a situation with
 zero occupancy of the deuterium nuclei in sites corresponding to
 $\text{N}^{\text{D}} \cdots \text{O}$

1 hydrogen bonding and 100 % occupancy in sites corresponding
2 to N D...N hydrogen bonding (across the temperature range
3 from 14 K to 288 K investigated in the powder neutron
4 diffraction study). Solid-state ^{15}N NMR data^[54] are also
5 consistent with the existence of N H...N hydrogen bonding in
6 this material.
7
8

3.3 Dynamic Properties

11 Although crystal structure determination from powder neutron
12 diffraction data gives a well-defined, ordered, time-averaged
13 structure, it is important to consider the possibility that
14 dynamic processes may occur in this material. In the case of
15 ammonium cyanate, it is also relevant to consider whether the
16 onset of the solid-state chemical transformation to produce
17 urea might be triggered by the occurrence of an appropriate
18 dynamic process of the ammonium cation.

19 With these motivations, we carried out a comprehensive
20 study of the dynamic properties of the ammonium cation in
21 solid ammonium cyanate,^[55] focusing on solid-state ^2H NMR
22 spectroscopy using the deuterated material (denoted ND_4^+
23 OCN^-) and incoherent quasielastic neutron scattering (IQNS)
24 using the material with natural isotopic abundances (denoted
25 $\text{NH}_4^+\text{OCN}^-$). The combination of these two techniques is a
26 powerful strategy for probing dynamic properties of organic
27 materials, as together they allow molecular motions to be
28 studied across a wide range of timescales. Relevant results
29 from a computational study^[56] of energy barriers for reorienta-
30 tion of the ammonium cation in ammonium cyanate are also
31 important in the context of deriving dynamic models for this
32 material.

33 A fundamental requirement of proposed models for
34 dynamic processes in crystalline solids is that the time average
35 of the dynamic process should be in agreement with the
36 crystal structure determined from diffraction-based studies. As
37 discussed above, powder neutron diffraction indicates that
38 there is no observable population of hydrogen/deuterium sites
39 corresponding to the orientation of the ammonium cation with
40 N H...O hydrogen bonding. Thus, any dynamic model that
41 implies a nonzero population of hydrogen/deuterium sites
42 corresponding to N H...O hydrogen bonding would be
43 incompatible with the experimental crystal structure. On this
44 basis, the following models (which preserve only N H...N
45 hydrogen bonds) were considered plausible.

46 Model A: 1808 jumps about one of the 2-fold axes of the
47 ammonium cation in the crystal structure. Starting from the
48 orientation with four N H...N hydrogen bonds, such jumps
49 take the ammonium cation into an equivalent orientation with
50 four N H...N hydrogen bonds.

51 Model B. 1208 jumps about one of the 3-fold axes of the
52 ammonium cation in the crystal structure, with one N H bond
53 (collinear with the rotation axis) remaining fixed during this
54 motion.

55 Model C. A 4-site tetrahedral jump model, in which each
56 hydrogen atom of the ammonium cation visits all four sites

(corresponding to the four N H...N hydrogen bonds) with equal probability during the timescale of the measurement. This situation could be achieved by individual jumps of the type discussed for model B (i. e., 3-site 1208 jumps about a single N H bond), but with the N H bond that serves as the rotation axis changing (on a time-dependent basis) such that each of the four N H bonds serves as the rotation axis with equal probability over the timescale of the measurement.

Solid-state ^2H NMR spectra, recorded as a function of temperature for a powder sample of deuterated ammonium cyanate, are shown in Figure 10, together with the simulated ^2H NMR line shapes for dynamic models A, B, and C. Visual comparison between experimental and simulated ^2H NMR line shapes strongly favours the tetrahedral jump model for the dynamics of the ammonium cation (Model C). As discussed in Section 2, finding the simulated ^2H NMR line shape that represents the best fit to the experimental ^2H NMR line shape at each temperature allows the jump rate to be established as a function of temperature, thus allowing activation parameters to be assessed. However, the fact that the experimental ^2H NMR line shape for ammonium cyanate is a single Gaussian line throughout most of the intermediate motion regime means that the fitting process to establish the jump rate that gives the best-fit line shape at each temperature is much less sensitive than usual. For this reason, analysis of ^2H NMR spin-lattice relaxation time data provides a more reliable quantitative determination of activation parameters for the motion.

The temperature-dependence of the powder-average ^2H NMR spin-lattice relaxation time $\langle 1/T_1 \rangle_p$, determined from 123 K to 290 K, is shown in Figure 11, together with a best-fit curve calculated for the tetrahedral jump model,^[57]

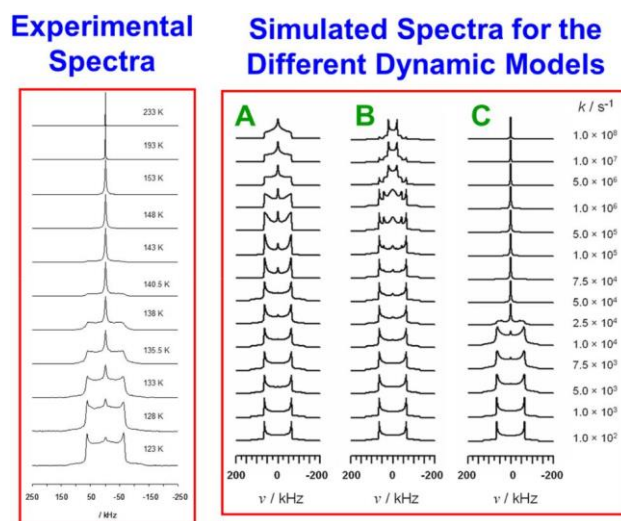


Figure 10. Left: Experimental solid-state ^2H NMR spectra recorded as a function of temperature for a powder sample of deuterated ammonium cyanate. Right: Simulated solid-state ^2H NMR spectra calculated for dynamic models A, B, and C defined in the text, for values of jump rate (k) ranging from the slow/static motion regime to the rapid motion regime.

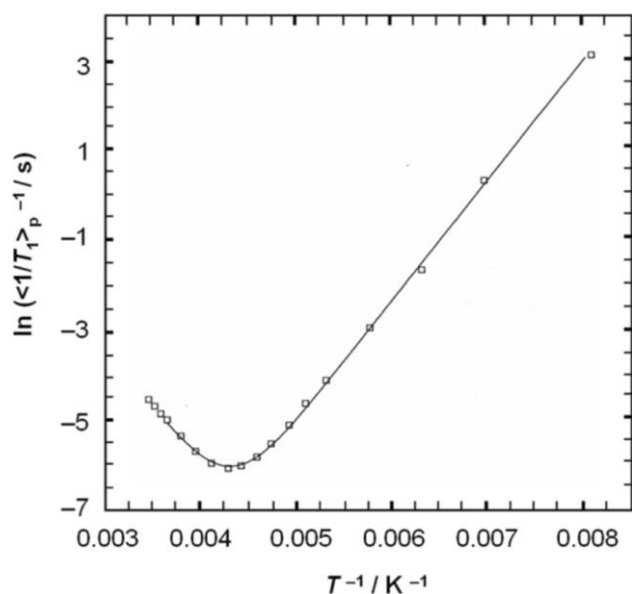


Figure 11. Temperature dependence of the powder-average ^2H NMR spin-lattice relaxation time $\langle 1/T_1 \rangle_p^{-1}$ for deuterated ammonium cyanate. The fitted line is the best fit to the experimental data using a theoretical expression for $\langle 1/T_1 \rangle_p^{-1}$ based on the tetrahedral jump model (model C). From the fitting process, the activation energy for 1.0 kJ mol

under the assumption that the temperature dependence of the jump rate exhibits Arrhenius behaviour. The three fitted parameters in this expression are the static quadrupole coupling constant (c), the activation energy (E_a) and the pre-exponential factor (t_c^0). The fitted theoretical expression is in excellent agreement with the experimental data, further supporting the tetrahedral jump model. The best-fit values of the activation parameters are: $E_a = (21.9 \pm 1.0)$ kJ mol $^{-1}$ and $\ln(t_c^0/s) = 31.3 \pm 0.8$. These results are in good agreement (within experimental errors) with those determined from IQNS data

[$E_a = (22.6 \pm 2.1)$ kJ mol $^{-1}$; $\ln(t_c^0/s) = 30.6$], which also provides strong support for the tetrahedral jump model in ammonium cyanate. It is important to emphasize the advantages of the combined strategy of using solid-state ^2H NMR spectroscopy and IQNS in the study of dynamic properties of organic solids, particularly as IQNS allows detailed characterization of motions that occur on shorter timescales than those that are accessible using solid-state ^2H NMR techniques.

3.4 Comments on the Solid-state Reaction of Ammonium Cyanate to Urea

Although the crystal structure of ammonium cyanate is now known and the dynamic properties are understood, a comprehensive study of the solid-state chemical reaction from ammonium cyanate to urea has not yet been reported, although possible insights derived from computational studies have

been proposed.^[58, 59] To address this issue, we are currently engaged in a detailed programme of research using a range of experimental techniques (including in situ powder X-ray diffraction and in situ solid-state NMR techniques) to gain a detailed understanding of kinetic and mechanistic aspects of this historically significant chemical reaction.

4. In Situ Solid-state NMR Strategies to Study the Evolution of Crystallization Processes

4.1 Introduction

Crystallization processes are encountered in many different scientific fields, and a deeper understanding of such processes has important practical implications, including the optimization of crystallization in industrial applications. Improving our fundamental mechanistic understanding relies on developing new experimental strategies, particularly those that allow direct in situ monitoring of the process.^[60] Crystallization processes are generally governed by kinetic factors and metastable solid forms often crystallize initially (rather than the thermodynamically stable form). Subsequently, the crystallization may evolve through a sequence of different transient solid forms before the final product is obtained. To optimize and control crystallization processes, it is essential to understand the sequence of events that occur in the evolution of the solid phase, rather than simply characterizing the final product recovered at the end of the process. Exploiting experimental strategies that allow direct in situ monitoring is clearly essential in pursuit of this aim.

We have recently focused^[61–66] on developing in situ solid-state NMR strategies for mapping the evolution of the solid phase during crystallization processes from solution. Here, we highlight the experimental method and present illustrative examples that reveal the types of information that can be obtained on the evolution of different solid forms (and interconversion between solid forms) during crystallization of organic systems from the solution state.

Importantly, the in situ solid-state NMR technique^[61] exploits the ability of NMR to selectively detect the solid phase in the types of heterogeneous solid/liquid system that exist during crystallization from solution, with the liquid phase “invisible” to the measurement. This technique has been shown to be a powerful approach for establishing the sequence of solid phases produced during crystallization^[62–64] and for the discovery of new (transient) solid forms.^[65]

4.2 The In Situ Solid-state NMR Technique

Until recently, the prospect of using solid-state NMR for in situ studies of crystallization from solution was limited by the difficulty of securely sealing a liquid phase inside an NMR rotor such that fast magic-angle sample spinning (MAS),

1 which is required for recording high-resolution solid-state
2 NMR spectra, can be carried out without problems arising
3 from leakage of the liquid from the rotor. Recently, suitable
4 rotor technology has been developed for sealing solutions
5 inside NMR rotors for MAS experiments, greatly facilitating
6 the development of the in situ solid-state NMR strategy
7 described here.

8 In our in situ solid-state NMR strategy for monitoring
9 crystallization (see Figure 12), a homogeneous (undersatu-
10 rated) solution is initially prepared inside the NMR rotor at
11 high temperature. Crystallization is induced by decreasing the
12 temperature rapidly to a target temperature at which the
13 solution is supersaturated, and hence crystallization is thermo-
14 dynamically favoured. The time dependence of the crystal-
15 lization process is then monitored by recording high-resolution
16 solid-state NMR spectra repeatedly as a function of time. The
17 time resolution of the in situ monitoring of the crystallization
18 process is dictated by the time required to record an individual
19 NMR spectrum of adequate quality to identify and distinguish
20 the different solid forms present during the evolution of the
21 system. Sufficiently good spectral resolution is also required
22 to identify and assign the solid phases present at different
23 stages of the crystallization process. Clearly, it is desirable to
24 be able to detect and identify the first solid particles produced
25 in the crystallization process, at which stage the amount of
26 solid in the system is generally very low. Thus, optimization
27 of the sensitivity of the measurement is also important,
28 allowing solid-state NMR spectra of adequate quality to be
29 recorded in the shortest possible time. To maximize the
30 sensitivity, isotopic labelling of the material to be crystallized
31 is desirable (although not always essential) and carrying out
32 the experiments at high magnetic field is advantageous.

33 A crucial feature of the strategy is that, by appropriate
34 choice of measurement conditions, solid-state NMR can give
35 complete selectivity in detecting only the solid component in
36 the system (and thus the dissolved solute and solvent are
37 undetected in the measurement). For organic materials, such
38 discrimination between solid and solution phases is readily
39 achieved by recording ^{13}C NMR spectra using the $^1\text{H}/^{13}\text{C}$
40 cross-polarization (CP) technique. As a consequence of differ-
41 ences in dynamic behaviour between molecules in the solid
42

and solution states, ^{13}C NMR spectra recorded using $^1\text{H}/^{13}\text{C}$
CP contain signals only from the solid phase. Thus, even if only
a small fraction of the solute has crystallized (e. g., in the early
stages of crystallization), only the solid particles contribute to
the measured NMR spectrum, and the dissolved solute (present
in a much higher amount in the early stages of crystallization)
and solvent are “invisible” to the measurement.

4.3 Example: Evolution of Different Solid Forms of Glycine During Crystallization from Solution

To illustrate the application of the in situ solid-state NMR
technique, we focus on studies of the crystallization of glycine
[$\text{H}_2\text{C}(\text{NH}_3^+)(\text{CO}_2^-)$] from different solvents. Under ambient
conditions, three polymorphs of glycine (denoted a, b, and g) are
known.^[67–71] The thermodynamically stable form is the g
polymorph, and the least stable form is the b polymorph.^[72, 73]
According to the literature, crystallization of glycine from water at
neutral pH produces the metastable a polymorph. However, a paper
published in 1961 suggested^[69] that crystallization of glycine from
deuterated water may promote the formation of the g polymorph,
although systematic studies of this isotope effect were only
reported recently,^[74, 75] in which it was demonstrated inter alia that
deuteration (even as low as 1 % deuteration) does significantly
increase the probability of obtaining the g polymorph. In high-
resolution solid-state ^{13}C NMR spectra, the isotropic ^{13}C chemical
shifts for the carboxylate carbon environment in the a, b, and g
polymorphs of glycine are 176.5, 175.5, and 174.5 ppm
respectively,^[76] allowing the three polymorphs to be readily
distinguished.

In the in situ ^{13}C NMR study^[62] of the crystallization of
glycine (for a sample ^{13}C -labelled in both carbon sites in the
molecule) from water with natural isotopic abundance (Figure
13a), a peak emerges at 176.5 ppm and the intensity increases
as a function of time. From the ^{13}C chemical shift, this solid
phase is assigned as the a polymorph. Thus, formation and
growth of the a polymorph is observed, consistent with the
literature, and no detectable amounts of the b or g polymorphs
are observed during the crystallization

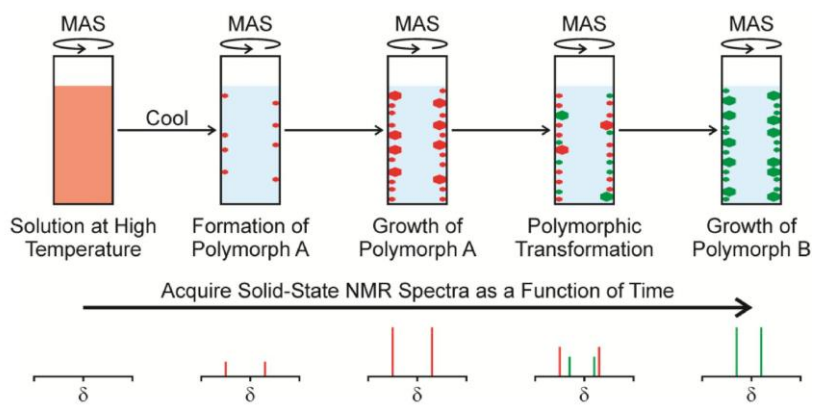


Figure 12. Schematic of the experimental strategy for in situ solid-state NMR studies of crystallization processes, illustrated for a system in which crystallization from solution initially produces a metastable polymorph A (red) followed by a polymorphic transformation to produce a more stable polymorph B (green). The corresponding changes in the high-resolution solid-state NMR spectrum, as a function of time, are shown at the bottom.

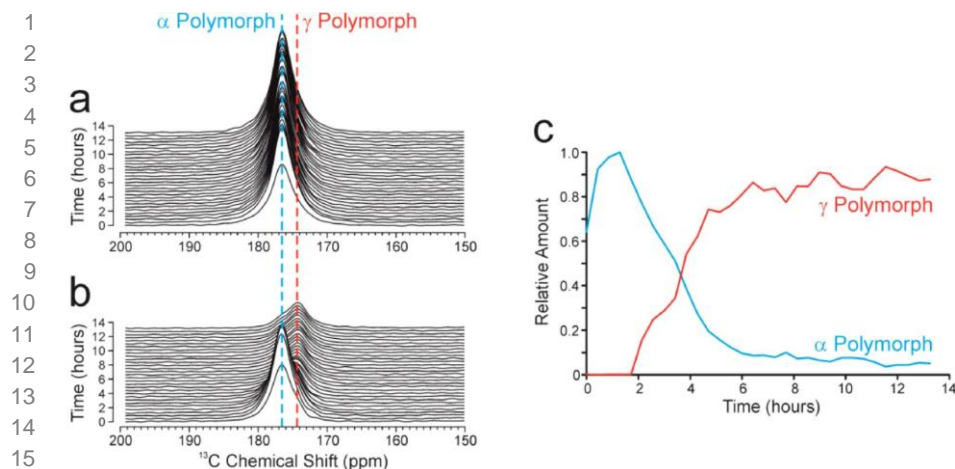


Figure 13. In situ solid-state ¹³C NMR spectra (showing only the carboxylate region) re-recorded as a function of time during crystal-lization of glycine from (a) H₂O and (b) D₂O.

(c) The relative amounts of the a polymorph (blue) and g polymorph (red) present, as a function of time, during crystallization from D₂O, established from the in situ solid-state ¹³C NMR data shown in (b).

experiment (which was carried out for a total time of 13 hr). We note that a comprehensive study of the crystallization of glycine from water^[75] (involving ex situ characterization by powder X-ray diffraction) has shown that the initially formed a polymorph eventually transforms to the thermodynamically stable g polymorph after a period of time that is typically of the order of several days.

To explore the isotope effect discussed above, crystallization of glycine (for a sample ¹³C-labelled in both carbon sites in the molecule) from deuterated water was studied.^[62] The total level of deuteration of all exchangeable hydrogen sites in the system (i. e., water molecules and NH₃⁺ groups of the zwitterionic glycine molecules) was 86 %. From the in situ solid-state ¹³C NMR results (Figure 13 b), it is clear that the a polymorph is again the first solid form produced in the crystallization process, suggesting that the same nucleation pathway is followed in both H₂O and D₂O. The amount of the a polymorph increases during the first 1.5 hr of the crystallization process. However, at this time, a new peak emerges at 174.5 ppm, characteristic of the g polymorph. The intensity of this new peak then increases with time, while the intensity of the peak due to the a polymorph decreases. The relative amounts of the a and g polymorphs present as a function of time, established from integrated peak intensities (corrected to allow for the different cross-polarization efficiencies of the a and g polymorphs), are shown in Figure 13 c. There is no evidence for any intermediate solid phase in the transformation from the a polymorph to the g polymorph, consistent with the rate of increase of the g polymorph mirroring the rate of decrease of the a polymorph (Figure 13 c). As discussed elsewhere,^[62, 64] the transformation from the a polymorph to the g polymorph during the evolution of the crystallization process is assigned as a solution-mediated polymorphic transformation, rather than a direct solid-solid transition.

For each of the two isotopomeric systems, the final polymorph obtained at the end of the in situ solid-state ¹³C NMR study (i. e., the a polymorph in the natural abundance system and the g polymorph in the deuterated system) is consistent with the preferred polymorphic outcome

observed in conventional (ex situ) laboratory crystallization experiments^[75] carried out under the same conditions and over the same total period of time.

Although a comprehensive understanding of the fascinating isotope effect in the crystallization of glycine from D₂O versus H₂O remains to be established, it is noteworthy that the way in which the crystal structures of the a and g polymorphs of glycine change upon deuteration is significantly different. Thus, it has been shown^[74] that the unit cell volume of the g polymorph decreases upon deuteration whereas the unit cell volume of the a polymorph increases upon deuteration, which could signify that the energy difference between the stable g polymorph and the metastable a polymorph may actually be greater for the deuterated system. However, we refrain from advancing this tentative thought until a rigorous theoretical analysis has been carried out.

It is relevant to note that, as with most of the important topics in structural chemistry, Jack Dunitz has explored^[77] the effects of deuteration on structural properties from the fundamental physicochemical viewpoint, and has applied his ideas in the case of crystalline benzene. In particular, this work demonstrated experimentally (from accurate neutron powder diffraction studies) and provided a fundamental rationalization of the fact that, below ca. 170 K, the volume per molecule in the crystal structure of deuterated benzene (C₆D₆) is lower than the volume per molecule in the crystal structure of benzene with natural isotopic abundances (C₆H₆), whereas above this temperature, the volume per molecule in the crystal structure of C₆D₆ is higher than that of C₆H₆.

The results from an in situ solid-state ¹³C NMR study of the crystallization of glycine from methanol/water^[63] are shown in Figure 14 (in this experiment, the glycine sample was ¹³C-labelled only in the carboxylate group, giving significantly narrower peaks than those in Figures 13 a and 13 b). In the first spectrum recorded, the solid phase is identified as a virtually pure sample of the b polymorph (a very small amount of the a polymorph is also present). Thus, the very early stages of crystallization yield a significant excess of the b polymorph in this system. Subsequently, the b

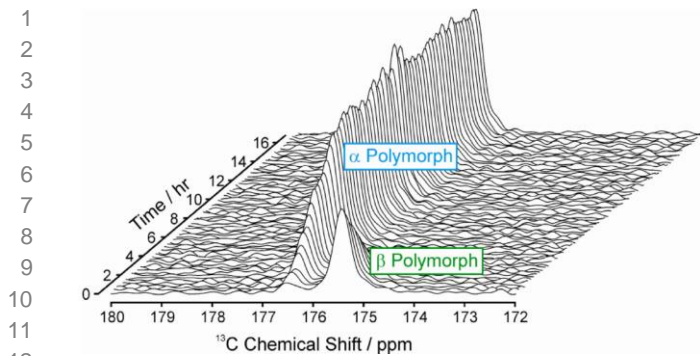


Figure 14. In situ solid-state ^{13}C NMR spectra (showing the carboxylate region) recorded as a function of time during crystallization of glycine from methanol/water.

polymorph transforms to the α polymorph by a solution-mediated transformation. Importantly, the results from our in situ solid-state ^{13}C NMR study allow the timescale of the transformation from the β polymorph to the α polymorph to be established, and indicate that a viable strategy for isolating the β polymorph would be to stop the crystallization experiment at the stage of the initial crystallization product, within only a few minutes of triggering the crystallization process.

4.4 Combined Solid-state and Liquid-state NMR Studies of Crystallization Processes

A recent development^[66] of the in situ NMR technique, with the potential to yield significantly deeper insights into crystallization processes than the version described above, exploits the fact that NMR can study both the liquid phase and the solid phase in a heterogeneous solid/liquid system using the same instrument, simply by changing the pulse sequence used to record the NMR data. Specifically, by alternating between two different pulse sequences in an in situ NMR study of crystallization, alternate solid-state NMR spectra and liquid-state NMR spectra are recorded, yielding essentially simultaneous information on the time evolution of both the solid phase and the liquid phase during the crystallization process. This strategy is called “CLASSIC NMR” (combined liquid- and solid-state in situ crystallization NMR). The CLASSIC NMR experiment creates the opportunity to elucidate the complementary changes that occur in the solid phase and in the liquid phase as a function of time during crystallization from solution. During the crystallization process, the changes in the amount and the identity of the solid phase are established from the time evolution of the solid-state NMR spectrum. Concomitantly, the solution phase becomes more dilute as the solid material is formed, and changes in the solution-state speciation and modes of molecular aggregation in solution are monitored from the time evolution of the liquid-state NMR spectrum.

In the case of the crystallization of *m*-aminobenzoic acid (*m*-ABA) from DMSO,^[66] the simultaneous use of both solid-state NMR and liquid-state NMR to probe the crystallization process has revealed significant insights (from the liquid-state data) into the nature of the supersaturated solution that exists prior to nucleation, in comparison with the equilibrium saturated solution that exists at the end of the crystallization process. In particular, in comparison with the final equilibrium saturated solution, the prenucleation supersaturated solution contains a significantly higher proportion of zwitterionic *m*-ABA molecules and/or a significantly higher proportion of nonzwitterionic *m*-ABA molecules, in which the amino group acts as a hydrogen-bond acceptor (e. g., in hydrogen-bonded clusters of *m*-ABA molecules). As the solid form produced in crystallization of *m*-ABA from DMSO is the zwitterionic polymorph I, it is clear that the existence in solution of zwitterionic *m*-ABA molecules and/or prenucleation clusters of nonzwitterionic *m*-ABA molecules engaged in intermolecular $\text{H}_2\text{N}\cdots\text{H}$ hydrogen bonding are very plausible precursors on the pathway to crystallization.

Clearly, the CLASSIC NMR experiment significantly extends the scope and capability of in situ monitoring of crystallization processes, as it is unique in providing simultaneous and complementary information on the time evolution of both the solid phase and the liquid phase. We fully anticipate that the advantages of the CLASSIC NMR strategy will yield significant new insights on a wide range of crystallization systems in the future.

4.5 Some Fundamental Considerations

4.5.1 What is the Smallest Size of Solid Particle that can be Detected in In Situ Solid-state NMR Studies of Crystallization?

An important question relates to the smallest size of solid particle that can be observed using the in situ NMR techniques described above, with implications on the earliest stage of the crystallization process that can be detected. As a basis for estimating the size limit,^[64] we recall (Section 4.2) that selective detection of the NMR spectrum only of the solid phase is achieved using the $^1\text{H}|^{13}\text{C}$ cross-polarization (CP) technique. The key limitation for obtaining a signal by CP is the rate of tumbling of the solid particle, as this motion “scrambles” the orientation of the dipolar couplings responsible for the polarization transfer. The tumbling motion is characterized by a correlation time (t_c) which is related to the volume (V) of the particle, the viscosity (η) of the solvent, and the temperature (T), through the Stokes-Einstein-Debye relation:^[78]

$$t_c \approx \frac{6 V \eta}{k_B T |\delta| \rho \Delta \rho},$$

where l is the order of the spherical harmonic for the

1 interaction ($l=2$ for dipolar coupling). Nowacka et al.^[79]
2 established that, for a $^1\text{H}|^{13}\text{C}$ CP experiment to give a signal
3 under similar conditions to those used in our experiments, the
4 limiting value of t_c is ca. 10 ms. Using the above equation and
5 taking the bulk viscosity of water (ca. 10^{-3} Pa s), the limiting
6 volume is estimated to be $V = 4 \times 10^{-7} \text{ \AA}^3$, corresponding to a
7 sphere with radius of ca. 210 \AA . To put this value in context,
8 particles of glycine of this size would contain around 5×10^5
9 molecules. Although some approximations are inherent in this
10 derivation, it nevertheless offers a reasonable estimate of the
11 smallest size of solid particle that could be detected in an
12 in situ solid-state NMR study of crystallization. Although the
13 size of the critical nucleation entity may vary significantly
14 between different systems and under different experimental
15 conditions, the critical nucleation clusters for organic crystals
16 are expected to comprise significantly less than 5×10^5
17 molecules. Thus, the smallest solid particles that can be
18 observed under the conditions of in situ solid-state NMR
19 studies using the $^1\text{H}|^{13}\text{C}$ CP technique are likely to represent
20 postnucleation stages of the crystallization process. We note
21 that, after observing the first peaks for the solid phase in our
22 in situ solid-state NMR studies of crystallization processes
23 using the $^1\text{H}|^{13}\text{C}$ CP technique, we do not observe any
24 evolution of the isotropic chemical shifts nor any evolution in
25 the peak widths as a function of time, which is consistent with
26 our conclusion that a signal is observed only for solid particles
27 that are sufficiently large to behave as the “bulk” solid.
28
29

30 **4.5.2 Does the NMR Measurement Technique Itself** 31 **Influence the Crystallization Process?**

32 Another important question is whether the rapid sample
33 rotation (MAS) required to record high-resolution solid-state
34 NMR spectra may actually influence the pathway and/or the
35 final outcome of the crystallization process, recognizing that
36 rapid sample spinning exerts a centrifugal pressure on the
37 sample. The pressure distribution within a sample subjected to
38 spinning in a cylindrical rotor is readily calculated if the
39 density distribution is known. Under typical conditions used in
40 in situ solid-state NMR experiments to study crystallization
41 processes, the induced pressure is estimated^[64] to be in the
42 region of 50–70 atm. As such pressures are significantly lower
43 than those typically required to induce transformations to
44 produce “high-pressure” polymorphs of organic materials, it is
45 unlikely that the pressure generated by MAS will induce
46 polymorphic transitions directly within the solid phase, except
47 in very rare cases.
48

49 However, it is more important to consider the effects of the
50 pressure induced by MAS on the solution phase properties of
51 the crystallization system. First, it is important to recognize
52 that rapid sample spinning induces a pressure gradient across
53 the cylindrical sample volume. The induced pressure is zero
54 on the rotation axis of the NMR rotor and increases radially
55 towards the walls of the rotor. In the case of a homogeneous
56 solution inside the rotor prior to crystallization, the solution

must respond to such a pressure gradient by redistribution of
mass towards the outer part of the rotor, creating a density
gradient across the sample (with lowest density at the centre of
the rotor and highest density at the walls). The existence of
such a density gradient may have important implications for the
ensuing crystallization process, particularly as it implies that
there may be a nonuniform distribution of concentration across
the solution. Furthermore, as solubility is a function of pressure,
the solubility may be different in different regions of the
sample. Clearly, the confluence of these factors may create a
significantly more complex crystallization environment than
that encountered in conventional laboratory crystallization
experiments. In our experience, however, we have not yet
observed any systems for which the final solid form extracted
from the NMR rotor following an in situ crystallization study
differs from the final solid form resulting from crystallization in
the laboratory under the same conditions and carried out over a
comparable period of time. However, we cannot rule out the
possibility that the effects of rapid sample spinning may
influence the pathway and outcome of the crystallization
process in some specific cases. We are currently embarking on
a programme of research to investigate the effects of rapid
sample spinning on solution behaviour from a deeper
physicochemical perspective.

Finally, we note that a previous study^[80] observed that the
polymorphic outcome of a solid-state dehydration process may
be influenced by the effects of rapid sample spinning in a solid-
state NMR experiment. For in situ solid-state NMR studies of
dehydration of sodium acetate trihydrate, the dehydration
process was found to produce a different distribution of the
polymorphs of anhydrous sodium acetate when dehydration
was carried out under conditions of rapid sample spinning
(leading to a mixture of polymorph I and polymorph beta of
anhydrous sodium acetate) compared with dehydration of a
static (nonspinning) sample under normal laboratory conditions
(leading to the formation of only polymorph beta of anhydrous
sodium acetate).

5. Future Challenges

As mentioned in Section 1, I believe that the most significant
and important challenge in structural chemistry in the next few
decades will be to derive a fundamental physicochemical
understanding of the process of crystal nucleation, and then,
based on this understanding, to devise experimental strategies
to enable crystallization processes to be controlled such that
they are directed towards very specific desired outcomes.

At present, a fashionable area of research is the computa-tional
prediction of all energetically reasonable crystal structures for a
given organic molecule.^[81–85] In many respects, however, the
results of such “crystal structure prediction” calculations, which
assess the energies of a large number of computer-generated crystal
structures, produce more questions than answers. Perhaps the most
significant issue is that crystal structure prediction calculations
typically generate a vast

1 number (perhaps even hundreds) of distinct crystal structures
2 within an energetically accessible range of the lowest-energy
3 structure, implying that all of these structures may be viable as
4 experimentally observable polymorphs. In the experimental
5 context, however, it is rare for an organic compound to exhibit

6 more than three or four known polymorphic forms, while
7 many organic compounds have only one experimentally
8 known crystal structure. So, why do crystal structure
9 prediction calculations generate so many plausible polymor-
10 phic forms, yet Nature appears to allow only a very small
11 subset of these polymorphs to arise in practice? Is this
12 situation a consequence of deficiencies in the computational
13 techniques? Or is it simply that not enough experiments have
14 been done under different crystallization conditions to allow
15 all the energetically accessible polymorphs to be found? Or is
16 it the case that many of the “unobserved” polymorphs are
17 actually produced during crystallization, but have a very facile
18 pathway to form a more stable polymorph (i. e., low barriers to
19 transformation on the energy landscape) and therefore have
20 only transitory existence during crystallization experiments
21 (perhaps with significantly shorter lifetimes than the transient
22 polymorphs revealed by the in situ solid-state NMR studies
23 discussed in Section 4.3)? Or, instead, does Nature impose
24 stringent rules governing crystallization pathways, such that
25 feasible pathways exist only for a very limited subset of the
26 energetically accessible bulk crystal structures predicted in the
27 calculations? While all of these possibilities may contribute to
28 the disparity between the computational predictions and
29 experimental reality, it is most likely that the disparity is a
30 consequence of our lack of understanding of the fundamental
31 factors that underlie crystallization processes, and in particular
32 our lack of detailed physicochemical knowledge of the critical
33 events that constitute crystal nucleation.

34 At present, we have a reasonably good understanding of
35 the nature of solution phases and the types of molecular
36 aggregation that may occur to form small molecular clusters
37 (for example, from solution-state NMR^[86] or computer-
38 simulation^[87] studies) of the type that might represent the very
39 earliest stages on the pathway towards crystallization. And we
40 already have a comprehensive understanding of the structural
41 properties and physical properties of the final “bulk” crystal-
42 line materials that represent the endpoints of crystallization
43 processes (from the extensive range of powerful diffraction-
44 based and spectroscopic techniques, some of which have been
45 discussed in earlier sections of this article). However, the
46 significant challenge is to fill the huge “knowledge void” that
47 exists between the earliest stages and the final stage of the
48 crystallization pathway. In particular, it is imperative to be
49 able to identify and understand the critical events that give rise
50 to crystal nucleation (representing the energy barrier that must
51 be surmounted for crystal growth to occur), and to unravel the
52 physicochemical factors that control crystal nucleation. Given
53 that our understanding of crystal nucleation is based, to a large
54 extent, on interpolating between our knowledge of the initial
55 stages and the final stage of the crystallization pathway, it is
56 not surprising that a number of different approaches for

rationalizing crystal nucleation have been proposed and are still
actively debated.^[88–92]

Experimental studies to observe and identify the critical
nucleation events in crystallization processes are challenging
for several reasons: 1) nucleation events are rare; 2) given that
critical nucleation entities are species of high energy on the
crystallization pathway, the population of such species is
inevitably low and the lifetime of such species is inevitably
short; 3) critical nucleation entities are likely to be in a size
regime that is inaccessible to most techniques for structural
analysis (i. e., significantly larger than small molecular clusters
of the type that may be observed and structurally identified by
traditional solution-state techniques, and significantly smaller
than the size of crystalline aggregates that may be observed and
structurally identified by traditional bulk solid-state
techniques), and 4) even if the sizes of critical nucleation
entities are accessible to experimental observation, it is likely
that, within the crystallization solution, there will be a much
higher population of (lower-energy) prenucleation entities and/
or a much higher population of (lower-energy) postnucleation
entities, such that to identify the critical nucleation entities from
among the mixture of particles of different sizes (each
representing a different point along the crystallization trajec-
tory) may be exceptionally difficult. Given these issues, the
current prospects for mapping the complete crystallization
pathway by experimental observation, including identification
of the critical events that correspond to crystal nucleation, are
inherently very challenging. Nevertheless, small but signifi-
cant steps of progress are being made by exploiting high-resolution
imaging techniques,^[93–95] in which clusters of the type that
may be important in nucleation are observed either by direct in
situ studies of the crystallization system (for example, by
liquid-phase transmission electron microscopy (TEM) or in situ
AFM) or through indirect ex situ studies (for example, by rapid
freezing of samples extracted from the crystallization system
followed by characterization using cryo-TEM techniques). We
note that, for certain systems, there may also be opportunities to
develop strategies to gain insights into the embryonic stages of
crystal growth processes by retro-spective analysis of fully
formed crystals recovered at the end of the crystallization
process.^[96]

From our present perspective and projecting into the future,
perhaps the most promising opportunity to observe a system on
the pathway towards nucleation and beyond, and hence
implicitly to identify the critical nucleation events, will be to
exploit computer-simulation techniques. One technical
challenge in this endeavour, however, is that ideally the
computer simulation should consider a system comprising a
sufficiently large number of molecules (to enable a reasonably
sized fragment of bulk crystal to be grown by the end of the
simulation) and should be run over a sufficiently long period of
time (to have a reasonable chance of observing an event as rare
as nucleation, and then to be able to follow the growth of the
fragment of bulk crystal beyond the nucleation event). In the
favourable case that a nucleation event does indeed occur
during the simulation, this approach will yield critical insights

1 into the structural changes (and the corresponding energetic
2 changes) that occur along the crystallization pathway, yielding
3 exquisite detail of the structural evolution towards nucleation,
4 and mechanistic details of the nucleation event itself.

5 Fortunately, recent progress towards the application of
6 computer-simulation methodologies to observe and understand
7 mechanistic aspects of crystal nucleation appears promis-
8 ing.^[97–102] Thus, as we look towards the horizon of present
9 capabilities and contemplate the range of fundamental insights
10 that we wish to discover, the prospects for exploiting
11 computer-simulation techniques to unravel the intricate and
12 complex details of crystallization pathways appear to provide
13 the most optimistic opportunities. And then, looking even
14 further into the future, once a sufficient level of fundamental
15 understanding of the physicochemical factors that control
16 crystal nucleation have been established, we will be in a
17 favourable position to exploit this understanding in formulat-
18 ing strategies to control crystallization pathways towards
19 achieving specific desired outcomes.

20 21 22 Acknowledgements

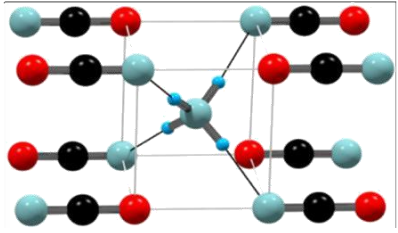
23
24 I am very grateful to many students, postdoctoral researchers,
25 and collaborators, past and present, who have contributed to
26 the research described in this article. Dr. Colan Hughes is
27 thanked for help in checking the manuscript.

28 29 30 31 32 References

- 33
34 [1] J. D. Dunitz, *X-ray Analysis and the Structure of Organic*
35 *Molecules*, Cornell University Press, Ithaca, 1979.
36 [2] K. N. Trueblood, J. D. Dunitz, *Acta Crystallogr. Sect. B: Struct.*
37 *Sci.* 1983, 39, 120.
38 [3] J. D. Dunitz, V. Schomaker, K. N. Trueblood, *J. Phys. Chem.*
39 1988, 92, 856.
40 [4] J. D. Dunitz, E. F. Maverick, K. N. Trueblood, *Angew. Chemie*
41 *Int. Ed. Engl.* 1988, 27, 880.
42 [5] J. D. Dunitz, *Pure Appl. Chem.* 1991, 63, 177.
43 [6] J. D. Dunitz, J. Bernstein, *Acc. Chem. Res.* 1995, 28, 193.
44 [7] J. D. Dunitz, *Acta Crystallogr. Sect. B: Struct. Sci.* 1995, 51,
45 619.
46 [8] K. D. M. Harris, *Top. Curr. Chem.* 2012, 315, 133.
47 [9] B. A. Palmer, G. R. Edwards-Gau, B. M. Kariuki, K. D. M.
48 Harris, I. P. Dolbnya, S. P. Collins, *Science* 2014, 344, 1013.
49 [10] J. M. Thomas, *Isr. J. Chem.* 2017, DOI: 10.1002/
50 *ijch.201600053*.
51 [11] D. C. Apperley, R. K. Harris, P. Hodgkinson, *Solid State NMR:*
52 *Basic Principles & Practice*, Momentum Press LLC, New York,
53 2012.
54 [12] M. J. Duer, *Introduction to Solid-State NMR Spectroscopy*,
55 Blackwell Publishing Ltd, Oxford, 2004.
56 [13] J. Seelig, *Q. Rev. Biophys.* 1977, 10, 353.
[14] L. W. Jelinski, *Ann. Rev. Mater. Sci.* 1985, 15, 359.
[15] R. R. Vold, R. L. Vold, *Adv. Magn. Opt. Reson.* 1991, 16, 85.
[16] G. L. Hoatson, R. L. Vold, *NMR* 1994, 32, 3.
[17] A. E. Aliev, K. D. M. Harris, *Struct. Bonding* 2004, 108, 1.
[18] R. W. G. Wyckoff, R. B. Corey, *Z. Kristallogr. Kristallgeom.*
Kristallphys. Kristallchem. 1934, 89, 462.
[19] P. Vaughan, J. Donohue, *Acta Crystallogr.* 1952, 5, 530.
[20] P. Vaughan, J. Donohue, *Acta Crystallogr. Sect. B: Struct.*
Crystallogr. Cryst. Chem. 1969, 25, 404.
[21] J. W. Emsley, J. A. S. Smith, *Trans. Faraday Soc.* 1961, 57,
1233.
[22] T. Chiba, *Bull. Chem. Soc. Japan* 1965, 38, 259.
[23] A. Zussman, *J. Chem. Phys.* 1973, 58, 1514.
[24] A. E. Aliev, S. P. Smart, K. D. M. Harris, *J. Mater. Chem.* 1994,
4, 35.
[25] S. J. Kitchin, S. Ahn, K. D. M. Harris, *J. Phys. Chem. A* 2002,
106, 7228.
[26] M. S. Lehmann, A. C. Nunes, *Acta Crystallogr. Sect. B: Struct.*
Crystallogr. Cryst. Chem. 1980, 36, 1621.
[27] M. S. Lehmann, T. F. Koetzle, W. C. Hamilton, *J. Cryst. Mol.*
Struct. 1972, 2, 225.
[28] J. D. Dunitz, A. Gavezzotti, *J. Phys. Chem. B* 2012, 116, 6740.
[29] S. J. Kitchin, G. Tutoveanu, M. R. Steele, E. L. Porter, K. D. M.
Harris, *J. Phys. Chem. B* 2005, 109, 22808.
[30] J. R. Long, B. Q. Sun, A. Bowen, R. G. Griffin, *J. Am. Chem.*
Soc. 1994, 116, 11950.
[31] Z. T. Gu, K. Ebisawa, A. McDermott, *Solid State Nucl. Magn.*
Reson. 1996, 7, 161.
[32] A. E. Aliev, S. E. Mann, A. S. Rahman, P. F. McMillan, F. Corà,
D. Iuga, C. E. Hughes, K. D. M. Harris, *J. Phys. Chem. A* 2011,
115, 12201.
[33] G. Ferguson, J. F. Gallagher, C. Glidewell, J. N. Low, S. N.
Scrimgeour, *Acta Crystallogr. Sect. C: Cryst. Struct. Commun.*
1992, 48, 1272.
[34] A. E. Aliev, E. J. MacLean, K. D. M. Harris, B. M. Kariuki, C.
Glidewell, *J. Phys. Chem. B* 1998, 102, 2165.
[35] H. Serrano-González, K. D. M. Harris, C. C. Wilson, A. E.
Aliev, S. J. Kitchin, B. M. Kariuki, M. Bach-Vergés, C.
Glidewell, E. J. MacLean, W. W. Kagunya, *J. Phys. Chem. B*
1999, 103, 6215.
[36] A. E. Aliev, C. E. Atkinson, K. D. M. Harris, *J. Phys. Chem. B*
2002, 106, 9013.
[37] M. Mella, K. D. M. Harris, *Phys. Chem. Chem. Phys.* 2009, 11,
11340.
[38] J. Kärger, D. M. Ruthven, *Diffusion in Zeolites and Other*
Microporous Solids, John Wiley & Sons, New York, 1992.
[39] H. Jobic, D. N. Theodorou, *Microporous Mesoporous Mater.*
2007, 102, 21.
[40] A. A. Khan, S. T. Bramwell, K. D. M. Harris, B. M. Kariuki,
M. R. Truter, *Chem. Phys. Lett.* 1999, 307, 320.
[41] A. E. Smith, *Acta Crystallogr.* 1952, 5, 224.
[42] K. D. M. Harris, J. M. Thomas, *J. Chem. Soc. Faraday Trans.*
1990, 86, 2985.
[43] M. D. Hollingsworth, K. D. M. Harris, in *Comprehensive*
Supramolecular Chemistry (Eds.: D. D. MacNicol, F. Toda, R.
Bishop), Pergamon, 1996, Volume 6, pp. 177–237.
[44] K. D. M. Harris, *Chem. Soc. Rev.* 1997, 26, 279.
[45] K. D. M. Harris, *Supramol. Chem.* 2007, 19, 47.
[46] J. Martí-Rujas, A. Desmedt, K. D. M. Harris, F. Guillaume, *J.*
Am. Chem. Soc. 2004, 126, 11124.
[47] J. Martí-Rujas, A. Desmedt, K. D. M. Harris, F. Guillaume, *J.*
Phys. Chem. B 2007, 111, 12339.
[48] J. Martí-Rujas, K. D. M. Harris, A. Desmedt, F. Guillaume, *J.*
Phys. Chem. B 2006, 110, 10708.
[49] J. Martí-Rujas, A. Desmedt, K. D. M. Harris, F. Guillaume, *J.*
Phys. Chem. C 2009, 113, 736.
[50] F. Wöhler, *Ann. Phys. Chem.* 1828, 12, 253.
[51] J. Liebig, F. Wöhler, *Ann. Phys. Chem.* 1830, 20, 369.

- 1 [52] J. Shorter, *Chem. Soc. Rev.* 1978, 77, 21.
2 [53] J. D. Dunitz, K. D. M. Harris, R. L. Johnston, B. M. Kariuki,
3 E. J. MacLean, K. Psallidas, W. B. Schweizer, R. R. Tykwinski,
4 *J. Am. Chem. Soc.* 1998, 120, 13274.
5 [54] E. J. MacLean, K. D. M. Harris, B. M. Kariuki, S. J. Kitchin,
6 R. R. Tykwinski, I. P. Swainson, J. D. Dunitz, *J. Am. Chem. Soc.*
7 2003, 125, 14449.
8 [55] A. Desmedt, S. J. Kitchin, K. D. M. Harris, F. Guillaume, R. R.
9 Tykwinski, M. Xu, M. A. Gonzalez, *J. Phys. Chem. C* 2008,
10 112, 15870.
11 [56] A. Alavi, R. J. C. Brown, S. Habershon, K. D. M. Harris, R. L.
12 Johnston, *Mol. Phys.* 2004, 102, 869.
13 [57] T. M. Alam, G. P. Drobny, *Chem. Rev.* 1991, 91, 1545.
14 [58] C. A. Tsipis, P. A. Karipidis, *J. Am. Chem. Soc.* 2003, 125,
15 2307.
16 [59] R. Méreau, A. Desmedt, K. D. M. Harris, *J. Phys. Chem. B*
17 2007, 111, 3960.
18 [60] N. Pienack, W. Bensch, *Angew. Chem. Int. Ed.* 2011, 50, 2014.
19 [61] K. D. M. Harris, C. E. Hughes, P. A. Williams, *Solid State Nucl.*
20 *Magn. Reson.* 2015, 65, 107.
21 [62] C. E. Hughes, K. D. M. Harris, *J. Phys. Chem. A* 2008, 112,
22 6808.
23 [63] C. E. Hughes, K. D. M. Harris, *Chem. Commun.* 2010, 46, 4982.
24 [64] C. E. Hughes, P. A. Williams, V. L. Keast, V. G. Charalampo-
25 poulos, G. R. Edwards-Gau, K. D. M. Harris, *Faraday Discuss.*
26 2015, 179, 115.
27 [65] C. E. Hughes, P. A. Williams, T. R. Peskett, K. D. M. Harris, *J.*
28 *Phys. Chem. Lett.* 2012, 3, 3176.
29 [66] C. E. Hughes, P. A. Williams, K. D. M. Harris, *Angew. Chemie*
30 *Int. Ed.* 2014, 53, 8939.
31 [67] G. Albrecht, R. B. Corey, *J. Am. Chem. Soc.* 1939, 61, 1087.
32 [68] Y. Iitaka, *Acta Crystallogr.* 1960, 13, 35.
33 [69] Y. Iitaka, *Acta Crystallogr.* 1961, 14, 1.
34 [70] P.-G. Jönsson, Å. Kvik, *Acta Crystallogr. Sect. B: Struct.*
35 *Crystallogr. Cryst. Chem.* 1972, 28, 1827.
36 [71] Å Kvik, W. M. Canning, T. F. Koetzle, G. J. B. Williams, *Acta*
37 *Crystallogr. Sect. B: Struct. Crystallogr. Cryst. Chem.* 1980, 36,
38 115.
39 [72] E. V. Boldyreva, V. A. Drebuschak, T. N. Drebuschak, I. E.
40 Paukov, Y. A. Kovalevskaya, E. S. Shutova, *J. Therm. Anal.*
41 *Calorim.* 2003, 73, 409.
42 [73] G. L. Perlovich, L. K. Hansen, A. Bauer-Brandl, *J. Therm. Anal.*
43 *Calorim.* 2001, 66, 699.
44 [74] C. E. Hughes, S. Hamad, K. D. M. Harris, C. R. A. Catlow, P. C.
45 Griffiths, *Faraday Discuss.* 2007, 136, 71.
46 [75] C. E. Hughes, K. D. M. Harris, *New J. Chem.* 2009, 33, 713.
47 [76] R. E. Taylor, *Concepts Magn. Reson. Part A* 2004, 22 A, 79.
48 [77] J. D. Dunitz, R. M. Ibberson, *Angew. Chemie Int. Ed.* 2008, 47,
49 4208.
50 [78] P. Debye, *Polar Molecules*, The Chemical Catalog Company,
51 New York, 1929.
52 [79] A. Nowacka, P. C. Mohr, J. Norrman, R. W. Martin, D.
53 Topgaard, *Langmuir* 2010, 26, 16848.
54 [80] M. Xu, K. D. M. Harris, *J. Am. Chem. Soc.* 2005, 127, 10832.
55 [81] A. Gavezzotti, *Acc. Chem. Res.* 1994, 27, 309.
56 [82] A. R. Oganov, C. W. Glass, *J. Chem. Phys.* 2006, 124, 244704.
[83] G. M. Day, *Crystallogr. Rev.* 2011, 17, 3.
[84] S. L. Price, *Acta Crystallogr. Sect. B: Struct. Sci. Cryst. Eng.*
Mater. 2013, 69, 313.
[85] S. L. Price, *Chem. Soc. Rev.* 2014, 43, 2098.
[86] A. Spitaleri, C. A. Hunter, J. F. McCabe, M. J. Packer, S. L.
Cockroft, *CrystEngComm* 2004, 6, 489.
[87] S. Hamad, C. E. Hughes, C. R. A. Catlow, K. D. M. Harris, *J.*
Phys. Chem. B 2008, 112, 7280.
[88] D. Erdemir, A. Y. Lee, A. S. Myerson, *Acc. Chem. Res.* 2009,
42, 621.
[89] R. J. Davey, S. L. M. Schroeder, J. H. ter Horst, *Angew. Chemie*
Int. Ed. 2013, 52, 2166.
[90] J. J. De Yoreo, P. U. P. A. Gilbert, N. A. J. M. Sommerdijk,
R. L. Penn, S. Whitelam, D. Joester, H. Z. Zhang, J. D. Rimer,
A. Navrotsky, J. F. Banfield, A. F. Wallace, F. M. Michel, F. C.
Meldrum, H. Cölfen, P. M. Dove, *Science* 2015, 349, aaa6760.
[91] D. Zahn, *ChemPhysChem* 2015, 16, 2069.
[92] Nucleation – a Transition State to the Directed Assembly of
Materials, *Faraday Discuss.* 2015, 179.
[93] J. Baumgartner, A. Dey, P. H. H. Bomans, C. Le Coadou, P.
Fratzl, N. A. J. M. Sommerdijk, D. Faivre, *Nat. Mater.* 2013, 12,
310.
[94] W. J. E. M. Habraken, J. Tao, L. J. Brylka, H. Friedrich, L.
Bertineti, A. S. Schenk, A. Verch, V. Dmitrovic, P. H. H.
Bomans, P. M. Frederik, J. Laven, P. van der Schoot, B.
Aichmayer, G. de With, J. J. De Yoreo, N. A. J. M. Sommerdijk,
Nat. Commun. 2013, 4, 1507.
[95] P. J. M. Smeets, K. R. Cho, R. G. E. Kempen, N. A. J. M.
Sommerdijk, J. J. De Yoreo, *Nat. Mater.* 2015, 14, 394.
[96] B. A. Palmer, K. D. M. Harris, F. Guillaume, *Angew. Chemie*
Int. Ed. 2010, 49, 5096.
[97] M. R. Walsh, C. A. Koh, E. D. Sloan, A. K. Sum, D. T. Wu,
Science 2009, 326, 1095.
[98] V. Agarwal, B. Peters, *Adv. Chem. Phys.* 2014, 155, 97.
[99] D. Gebauer, M. Kellermeier, J. D. Gale, L. Bergström, H.
Cölfen, *Chem. Soc. Rev.* 2014, 43, 2348.
[100] F. Giberti, M. Salvalaglio, M. Parrinello, *IUCrJ* 2015, 2, 256.
[101] Z. M. Aman, C. A. Koh, *Chem. Soc. Rev.* 2016, 45, 1678.
[102] G. C. Sosso, J. Chen, S. J. Cox, M. Fitzner, P. Pedevilla, A. Zen,
A. Michaelides, *Chem. Rev.* 2016, 116, 7078.

1
2
3
4
5
6
7
8
9
10
11
12
13
14
15
16
17
18
19
20
21
22
23
24
25
26
27
28
29
30
31
32
33
34
35
36
37
38
39
40
41
42
43
44
45
46
47
48
49
50
51
52
53
54
55
56



K. D. M. Harris*

1 – 18

Explorations in the Dynamics of
Crystalline Solids and the Evolution
of Crystal Formation Processes

